Available online at www.sciencedirect.com
SCIENCE DIRECT®
Journal of Electron Spectroscopy and Related Phenomena 137–140 (2004) 629–632
JOURNAL OF ELECTRON SPECTROSCOPY and Related Phenomena
www.elsevier.com/locate/elspec

Measurement of the electronic structure of crystalline silicon by electron momentum spectroscopy

M. Vos [a,*], C. Bowles [a], A.S. Kheifets [a], V.A. Sashin [a], E. Weigold [a], F. Aryasetiawan [b]

[a] *Atomic and Molecular Physics Laboratories, Research School of Physical Sciences and Engineering, Australian National University, Canberra 0200, ACT, Australia*
[b] *Research Institute for Computational Sciences, AIST, Tsukuba Central 2, Umezono 1-1-1, Tsukuba Ibaraki 305-8568, Japan*

Available online 28 March 2004

Abstract

Electron momentum spectroscopy (EMS) is a scattering experiment that determines the spectral function of a sample, i.e. the density of electrons as a function of binding energy and momentum. Here, it is used to study the spectral function of silicon single crystals in the extended zone scheme. Two symmetry directions and four intermediate directions are measured. The relation between the band index and the main observed momentum component is discussed. The observed peak shapes are compared with many-body calculations based on the cumulant expansion scheme. The dispersion is described well, but peak shapes agree with many-body theory only on a semi-quantitative level.

PACS: 71.20.Mq; 79.20.Kz

Keywords: Spectral function; Silicon; Band index; Electron correlation; Many body theory; Electron momentum spectroscopy

The measurement of properties directly related to the wave function of electrons provides a stringent test of our understanding of matter. In solids, photoemission has been used extensively to measure dispersion $\varepsilon_n(\boldsymbol{q})$, i.e. the dependence of the energy of a Bloch function $\phi_n(\boldsymbol{q})$ on its crystal momentum $\boldsymbol{q}$ (see [1]). Here, n is the band index. In the reduced zone scheme, the lowest band in energy is labelled 1, the next one 2, etc. The Bloch function is a linear combination of plane waves $\phi_n(\boldsymbol{q}) = \sum_G c_{\boldsymbol{G}}^n \, \mathrm{e}^{\mathrm{i}(\boldsymbol{q}+\boldsymbol{G})\cdot\boldsymbol{r}}$, where the summation extends over all reciprocal lattice vectors.

Electron momentum spectroscopy (an $(e, 2e)$ experiment at high momentum transfer) is a technique that determines more than just the dispersion $\varepsilon_n(\boldsymbol{q})$. In this technique, energetic incoming electrons ($E_0 = 50\,\mathrm{keV}$ in the present case, momentum $\boldsymbol{k}_0$) impinge on the target and some have a binary collision with a target electron and transfer a significant amount of their energy to this electron (here about half its energy). This struck electron is ejected from the target (a thin free-standing film), and both scattered and ejected electrons are measured in coincidence for both their energies E_1 and E_2 and momenta $\boldsymbol{k}_1$ and $\boldsymbol{k}_2$. Using the basic laws of energy and momentum conservation, one can (in an independent particle picture) calculate the binding energy ($\varepsilon = E_0 - E_1 - E_2$) and momentum ($\boldsymbol{p} = \boldsymbol{k}_1 + \boldsymbol{k}_2 - \boldsymbol{k}_0$) of the struck electron *before* the collision [2,3]. In the limit of an infinitely thin film, a specific Bloch function $\phi_n(\boldsymbol{q})$ contributes to the observed intensity distribution $I(\varepsilon, \boldsymbol{p})$ only at energy $\varepsilon(\boldsymbol{q})$ and only at momentum values $\boldsymbol{p} = \boldsymbol{q} + \boldsymbol{G}$ by an amount proportional to $|c_{\boldsymbol{G}}^n|^2$. We will show that the coefficients $|c_{\boldsymbol{G}}^n|^2$ can be determined by EMS. In this spectrometer, outlined in Fig. 1, the detectors are arranged in such a way that only target electrons with their momentum $\boldsymbol{p}$ directed along the y-axis can cause a coincidence. For more details, see [4].

For a target of finite thickness, multiple scattering has to be considered. The incoming or outgoing electrons can lose energy by inelastic collisions (e.g. plasmon excitation) and transfer momentum by elastic collisions (deflection from nuclei). These additional scattering events result in intensity appearing in the 'wrong' part of the spectrum, as either the energy balance or momentum balance equation is used incorrectly. For polycrystalline solids, these type of events can

* Corresponding author. Tel.: +61-2-6249-4985; fax: +61-2-6249-2452.
E-mail address: maarten.vos@anu.edu.au (M. Vos).

0368-2048/$ – see front matter © 2004 Elsevier B.V. All rights reserved.
doi:10.1016/j.elspec.2004.02.051

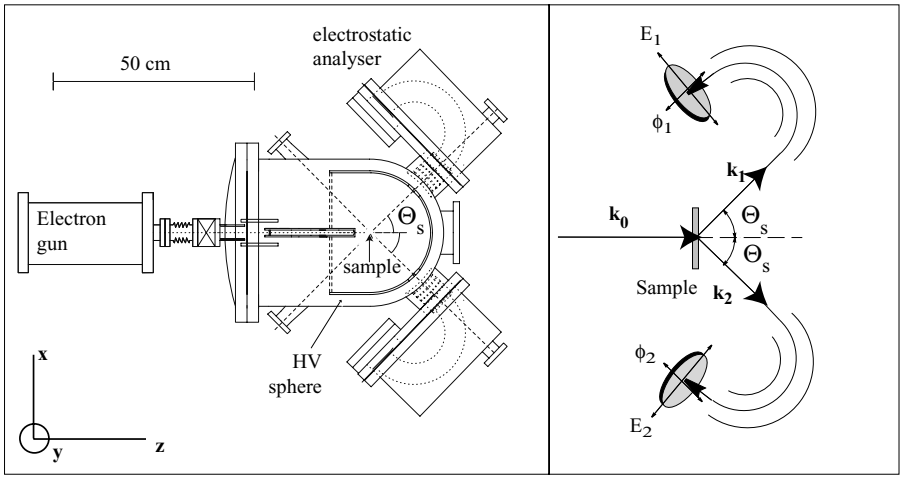

Fig. 1. An outline of the experimental set-up (left panel) and scattering geometry (right panel). An electron gun emits a well-collimated 25 keV electron beam. Upon entering the +25 kV high-voltage sphere (containing the target), the electrons are accelerated to 50 keV (and have a momentum $\boldsymbol{k}_0$). Electrons emerging from the target after a near symmetric $(e, 2e)$ event (with momentum $\boldsymbol{k}_1$ and $\boldsymbol{k}_2$) are analysed by the electrostatic deflectors, near ground potential.

be modelled by Monte Carlo simulations [5]. Alternatively, one can try to correct for inelastic multiple scattering only by measuring an energy loss spectrum of a 25 keV electron transmitted through the film and use this energy loss distribution to correct for inelastic scattering [6]. This approach is used later in the paper. In single crystal targets, elastic scattering often results in diffraction. As EMS measures the electronic structure as a function of momentum, rather than crystal momentum, diffraction affects the measurement in a meaningful way as it changes the observed magnitude of $|c_{\boldsymbol{G}}^n|^2$, i.e. the size of the contribution of different plane waves to the Bloch function.

For a free electron solid, the wave functions are plane waves and in the ground state the occupied states are within the Fermi sphere with radius k_f, i.e. $|\boldsymbol{k}| < k_\mathrm{f}$. This sphere is indicated as a dashed line in Fig. 2. The lattice potential of silicon can be considered as a perturbation, changing the free electron picture. Now the wave functions are Bloch functions with, for each solution, more than one $|C_{\boldsymbol{G}}^n|^2 > 0$. Silicon is a semiconductor with eight electrons per unit cell, and hence in the ground state the first four bands are fully occupied (one spin up and one spin down electron per band). In Fig. 2, we show a cut of the reciprocal lattice along the $p_z = 0$ plane and the first four Brillouin zones. We now want to discuss the results of the measurement of silicon and emphasise that band n has maximum intensity in Brillouin zone n.

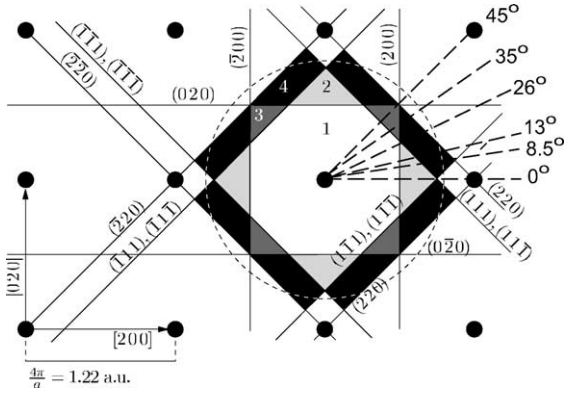

Fig. 2. The cut through the reciprocal lattice of silicon at $p_z = 0$. The first four Brillouin zones are indicated. The Brillouin zone boundaries are labelled by the indices of the reciprocal lattice it bisects. The dashed circle is the Fermi sphere of a free electron solid with the same electron density as silicon. Different measurement directions are indicated by dashed lines.

In EMS, the incoming and outgoing electrons are to a good approximation plane waves. The measurement method does not depend on the crystal lattice, indeed it works as well for atoms, molecules and amorphous materials as it does for crystals. Hence, one can measure the ϕ_n for any momentum direction. In our set-up, we can rotate the sample around the surface normal which coincides with the z-axis (incoming beam direction) of the spectrometer. Here, the sample was a thin ($\simeq$20 nm) silicon crystal with $\langle 0\,0\,1\rangle$ surface normal, see [7] for sample preparation details. Diffraction spots of the transmitted beam were observed at a phosphor screen reflecting the sample alignment. The sample was aligned with the spectrometer y-axis (the measurement direction) aligned with the $\langle 1\,0\,0\rangle$ direction, the $\langle 1\,1\,0\rangle$ direction and four intermediate directions (see Fig. 2).

Linear muffin tin orbital (LMTO) calculations, with the results split out for the four occupied bands, were done for the same directions. All calculations were broadened with the experimental 1 eV energy resolution. The results are plotted in Fig. 3 together with the experimentally observed distributions.

For the measurement of momenta directed along the $\langle 1\,0\,0\rangle$ direction the theory predicts band 1 and 2 occupied. In the first Brillouin zone, band 1 is occupied, changing abruptly to band 2 at 0.61 a.u. The dispersion shows no band gap while crossing the first Brillouin zone. The absence

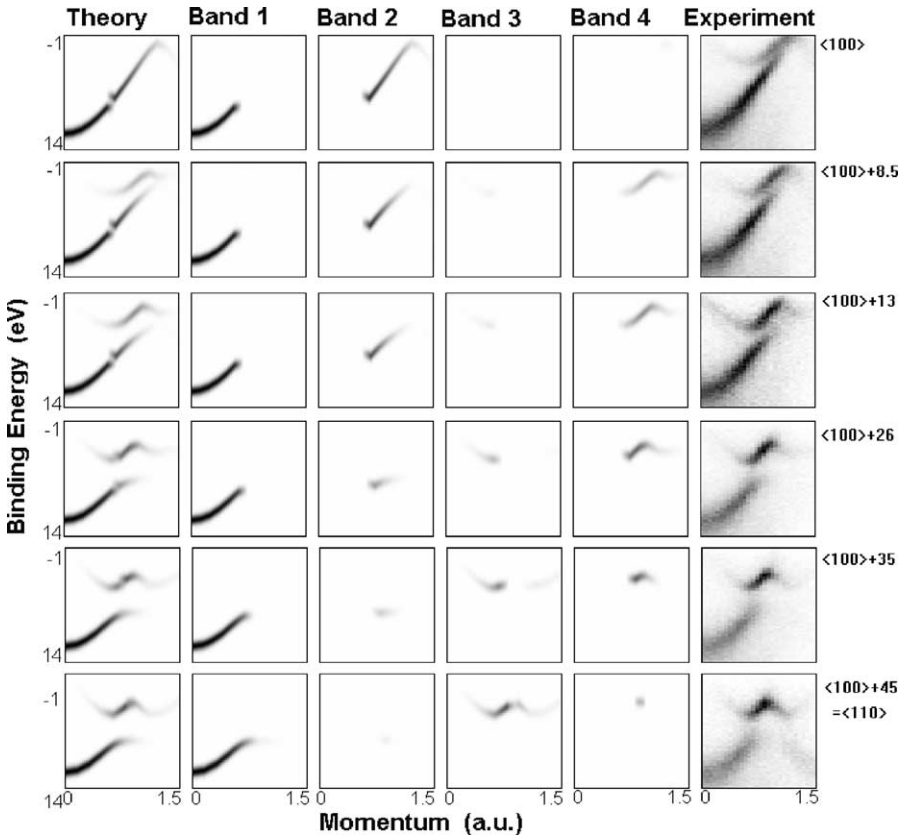

Fig. 3. The LMTO calculated band structure (total and split up for the contributions of bands 1–4) for the different directions indicated in Fig. 2 compared with the measured results.

of a band gap here is a peculiarity of the diamond lattice related to additional symmetry (see [8]). After leaving the second Brillouin zone, the calculated intensity drops only gradually to zero. The same behaviour is seen in the measured intensity (right panel), but an additional branch is observed as well, at smaller binding energy and merging with the main feature at 1.2 a.u. Calculations for the crystal rotated by 8.5° show the same branch as well, and it belongs to band 4. From the shape of the Brillouin zone it is clear that the measurement along the ⟨1 0 0⟩ direction just misses Brillouin zone 4 (see Fig. 2). Due to finite momentum resolution, and possibly small misalignments, it is inevitable that the ⟨1 0 0⟩ measurements samples Brillouin zone 4 as well and this will cause the extra branch in the observed intensity. In the ⟨1 1 0⟩ symmetry direction, the first Brillouin zone crossing is with two planes, (the (1 1 1) and (1 1 $\bar{1}$) planes, making an angle of ±54.35° with the $p_z = 0$ plane). Thus, the band index switches from 1 to 3 after the double crossing. Now we see the classic band gap behaviour, band 1 has a minimum in binding energy at the Brillouin zone crossing, and peters out after the crossing. Band 3 slowly increases in intensity from zero momentum up to the first Brillouin zone boundary, and has a maximum in binding energy there. The next extremum in the energy (a minimum in binding energy) is when band 3 crosses the next set of Brillouin zone boundaries, and its intensity drops for larger momenta, i.e. after leaving Brillouin zone 3. Indeed, the experiment resembles the calculations. For the intermediate directions, there is a large contribution of band 4 for directions not too far from the ⟨1 0 0⟩ direction, and large contributions from band 3 for directions approaching ⟨1 1 0⟩. Thus, the plot of the Brillouin zone (Fig. 2) can be used as a rough guide to understand which bands contribute intensity. The measured intermediate spectra show the same progression as the theory.

However, even from these semi-quantitative grey-scale presentation it is clear that the measured intensity does not follow the observed intensity. The LMTO theory predicts the maximum intensity near the bottom of the band, whereas the experiment has maximum intensity at intermediate binding energies, or even near the top of the band. This is due to life-time broadening not incorporated in the LMTO theory. Examination of the observed spectra shows not only line broadening but also asymmetries. We performed full-scale many-body calculations in an attempt to describe the data more quantitatively. Calculations based on the *GW*-approximation [9] and on the cumulant expansion approximation [10] were done. The *GW*-calculation produced satellites at larger binding energies, that were not observed in the experiment. The cumulant expansion calculation did not have distinct satellites, but produced similar (but weaker) asymmetries of the peaks as seen in the experiment.

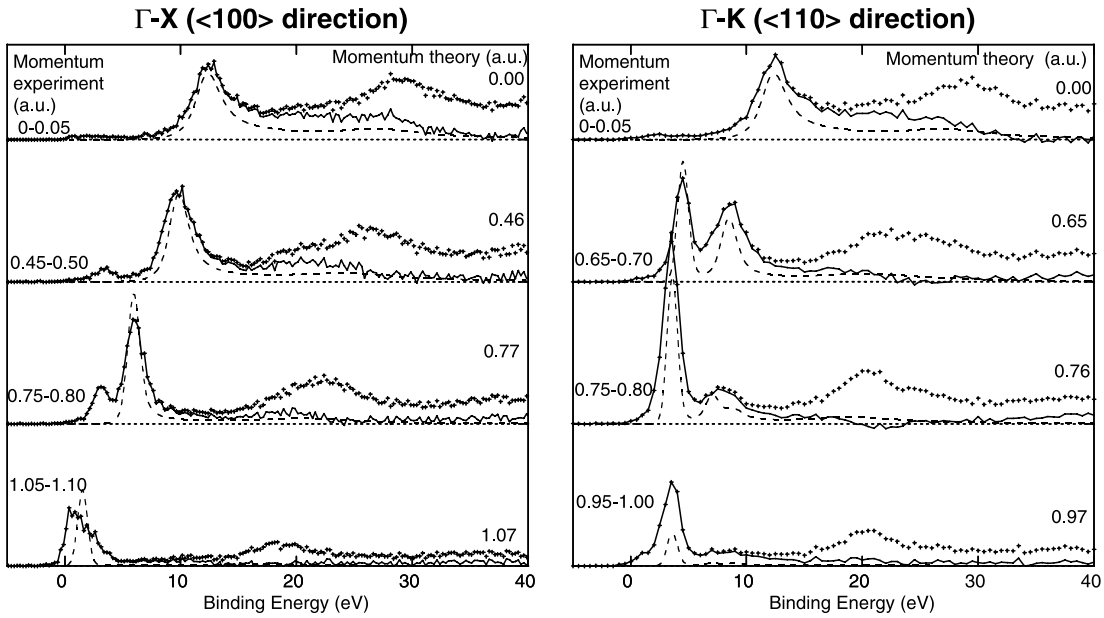

Fig. 4. Spectra at selected momenta along the $\Gamma - X$ (left panel) and $\Gamma - K$ (right panel) direction (dots: raw experimental data; solid line: deconvoluted for inelastic multiple scattering effects using the measured energy loss distribution as described in [6]). The dashed line is the result of the cumulant expansion calculation. For each panel, only a single normalisation constant has been used to scale the intensity of the theory to the measured intensity.

The cumulant expansion calculation is plotted in Fig. 4 together with the experiment. The agreement is good but not perfect, an encouraging fact as a truly quantitative comparison between a representation of the wave function and experimental data has the potential of creating new levels of understanding.

References

[1] S. Hüfner, Photoelectron Spectroscopy, Springer, Berlin, 1995.
[2] E. Weigold, I.E. McCarthy, Electron Momentum Spectroscopy, Kluwer Academic Publishers/Plenum Press, New York, 1999.
[3] M. Vos, I.E. McCarthy, Rev. Mod. Phys. 67 (1995) 713.
[4] M. Vos, G.P. Cornish, E. Weigold, Rev. Sci. Instrum. 71 (2000) 3831.
[5] M. Vos, M. Bottema, Phys. Rev. B 54 (1996) 5946.
[6] M. Vos, A.S. Kheifets, E. Weigold, in: D.H. Madison, M. Schulz (Eds.), Correlations, Polarization and Ionization in Atomic Systems, Proceedings of the IAP Conference, vol. 604, American Institute of Physics, New York, 2002, pp. 70–75.
[7] S.J. Utteridge, V.A. Sashin, S.A. Canney, M.J. Ford, Z. Fang, D.R. Oliver, M. Vos, E. Weigold, Appl. Surf. Sci. 162–163 (2000) 359.
[8] V. Heine, Group Theory in Quantum Mechanics, Pergamon Press, New York, 1960.
[9] L. Hedin, J. Phys: Condens. Matter 11 (1999) R489.
[10] F. Aryasetiawan, L. Hedin, K. Karlsson, Phys. Rev. Lett. 77 (1996) 2268.